Chapter 5

Preparation of the joints and welding process

5.1 YBCO/Ag composite

$YBa_2Cu_3O_{7-\delta}$ superconductor oxides are expected for high critical current applications. The melt processes are effective for obtaining highly aligned YBCO crystals and, thus, high critical current densities. Unfortunately, these materials are inherently brittle due to their ceramic character resulting in limited mechanical strength. Several studies [4, 5, 59, 60] have confirmed that Ag addition has a positive influence on the mechanical strength and cracking resistance of YBCO melt processed bulk superconductors. This has caused a strong interest in the potential use of these materials in trapped field applications, where strong magnetic forces induce material cracking and, hence, limit the maximum trapped field [61, 62]. In figure 5.1a can be seen that by increasing the quantity of Ag into YBCO matrix until a pseudo-monotectic composition which is 5% from total weight of the sample the peritectic temperature is decreased up to 970°C. This temperature is kept constant with further Ag addition. Silver was shown not to degrade the properties of YBCO and although the processing temperature of YBCO was significantly higher than the melting point of silver, liquid silver was retained behind the advancing solid-liquid interface during the solidification process [63]. This indicated that liquid silver had very low solubility in the

$BaCuO_2$-CuO liquid from which YBCO was growing.

Ag is dispersed in these superconductors in the form of droplets, the size, the shape and distribution of which depend on solidification conditions. To control these parameters, studies of the YBCO/Ag composites phase diagram [3,4,5,64] morphology and growth mechanisms have been performed [4,5,64].

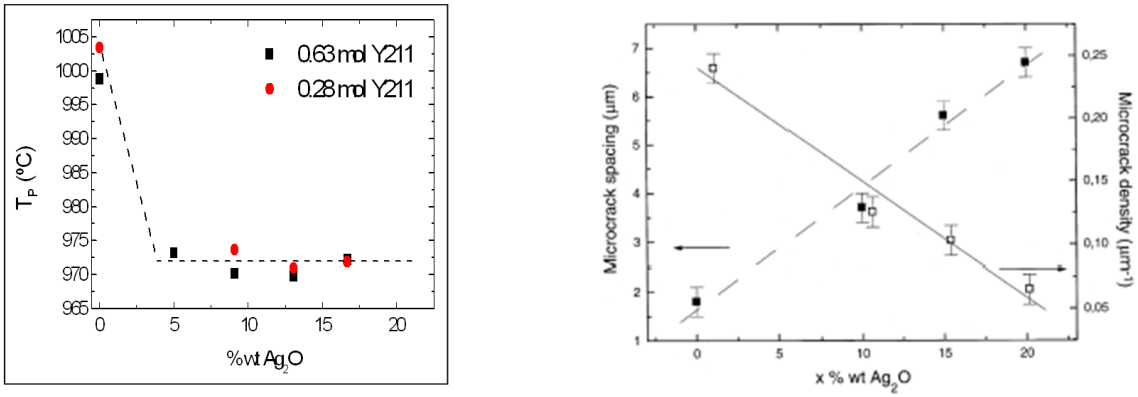

(a) (b)

Figure 5.1: a) Peritectic temperature of the melt-textured YBCO-Ag composite as a function of Ag_2O addition; b) Microcrack spacing (■) and microcrack density (□) as a function of A_2O content in the starting mixture.

Mendoza *et al.* [5] have observed two main morphological effects when they add Ag to the YBCO matrix. First, the porosity normally observed in top seeding samples, has completely disappeared. Second, the mean distance between the microcracks lying parallel to the ab planes, i.e. microcrack spacing, has strongly increased. In figure 5.1b can be seen that the microcrack spacing linearly increases by increasing the percentage of A_2O addition. Results of the microcrack density dependence on the A_2O addition are also shown in figure 5.1b. The microcrack density decreases linearly with the A_2O addition, thus confirming a strong correlation between Ag addition and the reduction of the microcrack density. It is expected that, if the microcraks density is reduced, the superconducting properties are increased. Moreover, Mendoza *et al.* have studied the influence of Ag content on the critical current density. Thus, they have reported that the

critical current density and the irreversibility line are strongly increased. Critical current densities (J_c^{ab}) up to $2.5 \cdot 10^6 A/cm^2$ at zero field and 5K and up to $2 \cdot 10^4 A/cm^2$ at zero field and 77K can be understood as a direct consequence of the microcrack density reduction.

The spacing of both a-b microcracks and c-cracks were measured also by P.Diko *et al.* [59]. Results of these experiments show that silver particles significantly suppressed both a-b and c-cracking. Change in a-b cracks spacing caused by Ag addition is comparable with the values reported by Mendoza *et al.* [5]. This finding is significant with respect to superconducting as well as mechanical properties of the melt-textured growth YBCO monoliths. Additionally, the reduction of microcrack spacing can be interpreted also as a consequence of the very high plasticity of Ag precipitates (very low yielding stress). Thus, the propagation of the micro and macrocracks is suppressed when they encountered Ag particles, thus improving the resistance against crack propagation in the YBCO/Ag bulk.

5.2 Welding process

Optimum performance of the joint at the interface region can be expected if the region reveals a similar microstructure as the YBCO/Ag melt textured bulk, and -more importantly- with no impurities at the junction. During the joining process the nucleation is different to that of seeded melt texturing of bulk YBCO. In the top seeded growth process the seed crystal essentially generates a controlled oriented point nucleus in the bulk, which further grows according to its habitual path along the c-axis and ab planes without any spatial constrains in the bulk. During the joining process the conditions are different in terms of both, the nucleation mechanism and spatial constraints. By inserting a Ag-based material between two YBCO single domains, at a temperature higher than the T_p of YBCO/Ag composite and lower than the T_p of YBCO material, Ag diffuses into the YBCO material and generates the melting of the YBCO material if the quantity

of Ag into the YBCO matrix exceeds 5%wt. For instance, the entire growth process is constrained to the molten region which depends on the growth conditions and, thus, on the Ag diffusion lengths. Unlike the point nucleus in top seeded melt growth, during the joining process the Y123 phase sympathetically nucleates on the entire surface of the joining blocks. This occurs simultaneously on both surfaces of YBCO blocks, generating basically two competing growth fronts growing towards each other. This further limits the spatial growth of the individual YBCO growth fronts to half of the joining region, if the Ag diffusion in both YBCO blocks is extended to the same lengths.

Thus, the process for the fabrication of artificial joints between YBCO ceramics is based on the knowledge of the high temperature phase diagram of the YBCO-m%Ag composites [3]. As it was mentioned, when m lies between 5 and 20 % in weight in these composites, the peritectic temperature of YBCO/Ag composite is decreased by about 40°C when the process is operated at atmospheric pressure [3]. It will be very practical, then, to induce the interfacial melting of two bulk YBCO single crystal ceramics if we insert some Ag near the surface. In this way we control the Ag diffusion into the YBCO crystals and we govern the solidication process of YBCO material previously molten due to the Ag diffusion.

In figure 5.2 are represented the steps that we have followed in order to obtain the superconducting joints studied in this work. Single domain $YBa_2Cu_3O_{7-\delta}$ monoliths were grown by Top Seeding Growth Method using Nd123 seeds [65, 66]. The pieces to be welded were cut using a diamond saw perpendicular to the ab plane and the surfaces in contact (ac planes) are polished carefully to improve their mechanical contact during the welding process.

In a separate process Ag-based welding agent with a predetermined thickness is prepared and cut with the dimensions of the YBCO surfaces to be joined. The Ag based material is inserted between both YBCO surfaces and the whole structure YBCO/Ag/YBCO is held in contact during the high temperature process, but without the need to apply some pressure, only that required to maintain the

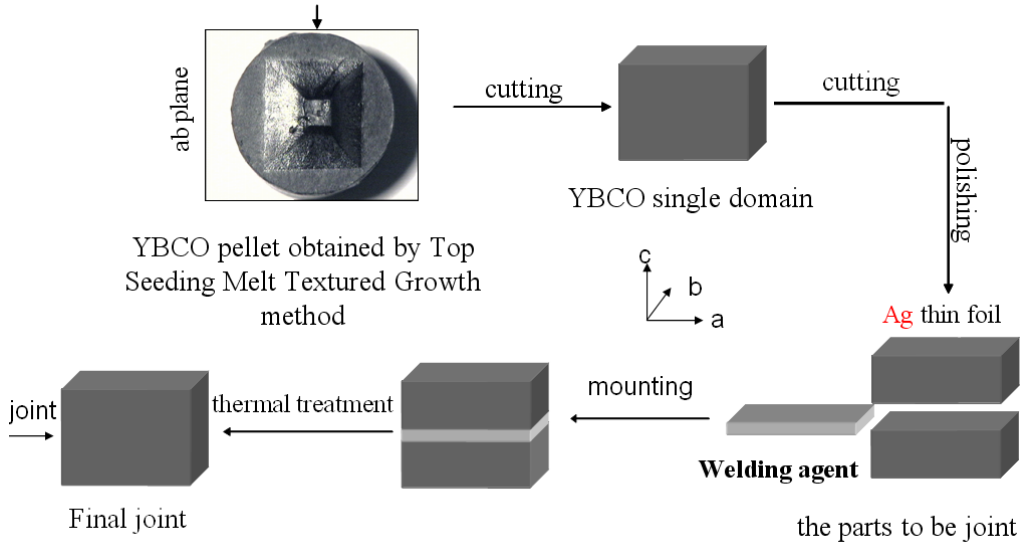

Figure 5.2: Steps to follow for the preparation of YBCO/Ag/YBCO joints: the single domain to be joint is extracted from an YBCO pellet obtained by top seeding melt textured growth method. Then, is cut perpendicular to the ab plane so that the Ag based welding agent is inserted between two ac planes. The Ag based welding agent is obtained by a standard rolling process if a Ag foil is used or by suspension in acetone if a Ag_2O powder is used and the thickness used in this study is spanning between 10 and 100 μm. Finally the assembly is submitted to thermal process and a clear and incident superconducting joint is obtained.

whole set assembled together. We have observed that without the system used to subject the assembly, the contact between the three parts is not good and the quality of the final joints is decreased. In this direction, Noudem *et al.* [67] have observed that the existence of a gap between the joining faces is not favorable for the quality of the joint. It will lead to non-beneficial effects on the texturing process such as loss of the liquid phases from the molten interface. This kind of effects degrade the texturing process. Once prepared, the assembly is subjected to a high-temperature process for the self seeding process.

Figure 5.3 shows a schematic illustration of the experimental setup used in a high temperature furnace. To achieve an isothermal region around the sample, it was placed inside a silicon carbide tube which behaves as a thermal shield. The temperature was monitored by two thermocouples set close to the welding

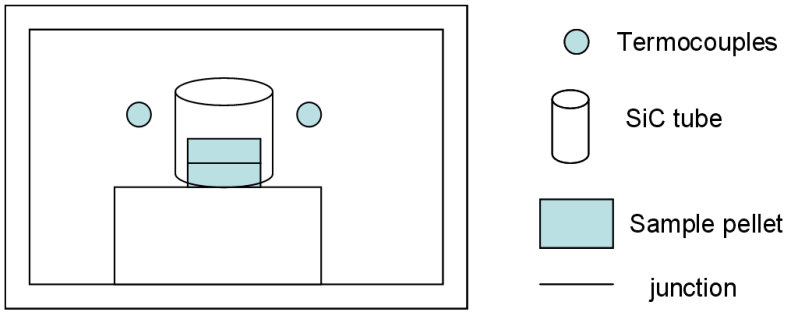

Figure 5.3: Schematic illustration of the experimental setup. The temperature of the furnace was monitored by two termocouples situated close to the sample. For the high temperature process, the assembly was surrounded by a silicon carbide tube in order to achieve an isothermal region around the sample. The junction is situated in the horizontal direction.

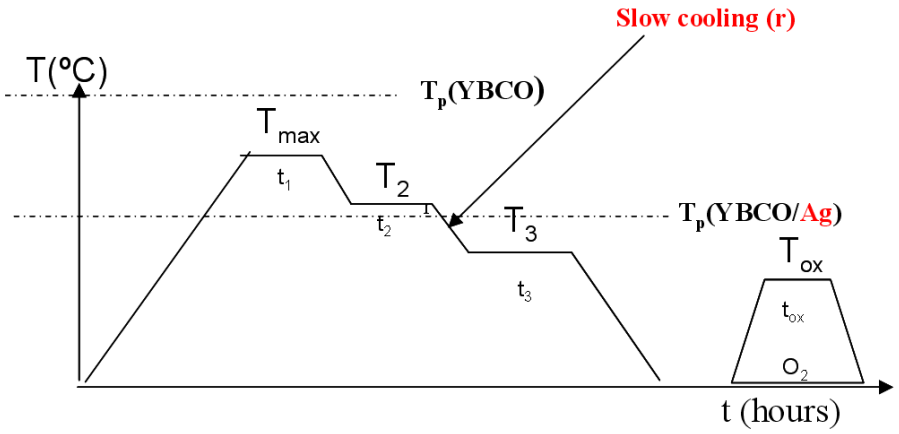

Figure 5.4: General schema of the thermal cycle followed to fabricate a superconducting joint. The temperatures T_{max}, T_2 and T_3 can be varied within a certain range depending on the microstructure of the initial YBCO ceramics. T_{ox} and t_{ox}, where T_{ox} is the maximum temperature of the oxygenation process and t_{ox} is the time spent by the sample at T_{ox}, must be optimize in order to reestablish the superconducting behavior of the final joints.

arrangement. The thermal cycle used to obtain high quality superconducting joints is schematically represented in figure 5.4.

The high temperature process has been performed for all samples studied in this work in air. In this thermal cycle we can distinguish four different temperatures which are critical for the final quality of the joint: T_{max}, T_2, T_3 and T_{ox}. T_{max}

is the maximum temperature reached during the thermal cycle. T_2 and T_3 determine a temperature window ΔT, where the ceramic assembly is slowly cooled at a rate r to induce a seeded crystallization of the melted interface. T_{ox} is the oxygenation temperature to which the final joint is subjected to reestablish the superconducting behavior.

Thus, the assembly is heated up to T_{max} and maintained during a holding time t_1 to achieve an homogeneous melt of the YBCO interfaces. At this temperature, Ag melts and slightly diffuses into the YBCO solid generating a molten interface. The Ag penetration depth can be controlled by the initial thickness of the Ag based agent and thermal treatment. Then, the sample is cooled down rapidly until T_2, which is a temperature slightly above the melting point of YBCO/Ag composite (970°C) and it is held for a time t_2. During all this time the YBCO/Ag interface is kept in the liquid state. The sample, is slowly cooled down until T_3, which is a temperature above the homogeneous nucleation of YBCO/Ag composite, inducing through a self-seeded process a crystallographically and chemically clean interface. Once the interface solidifies, the assembly is fast cooled with a rate of 205°C/h down to the room temperature.

The high-temperature process reduces the oxygen level from the sample and has a tetragonal structure. As it is known, only the orthorhombic structure is superconducting, as a consequence, an additional process in oxygen atmosphere is needed for the establishment of the superconducting behavior. For an homogeneous oxygenation the temperature T_{ox} and the time t_{ox} are important parameters and must be controlled. These parameters depend on the size of the sample to be oxygenated and its microstructure. In the tetragonal to orthorhombic transformation, the crystalline structure changes and stresses can be produced in the sample. For instance, during this process micro and macrocracks can appear.

For the optimization of the welding process, parameters such as: maximum temperature of welding process (T_{max}), the time spent by the joint at the max-

imum temperature (t_{melt}) welding configuration, window temperature (ΔT), Ag based welding agent thickness, oxygenation time (t_{ox}) and cooling rate (r) have been studied.

5.3 Ag based welding agents

In this section will be presented a basic characterization of the final joints obtained by the welding process explained before and using different Ag-based welding agents. We have used: a Ag_2O powder obtained by suspension in acetone and a Ag thin foil obtained by a cold rolling process as welding agents. The characterization consists of analyzing the microstructure and physical properties of the final joints such as: remanent magnetization after a fc process, temperature dependence of the resistivity measured at different applied magnetic field and, finally, the irreversibility line of both, YBCO monoliths and final joints. The microstructure has been evaluated by means of scanning electronic microscopy, whereas the remanent magnetization after a fc process was determined by means of in-field Hall probe imaging measurements. The temperature dependence of the resistivity at different applied magnetic fields of both, YBCO monolith and final joint, has been determined by transport measurements by using a PPMS (Physical Properties Measurement System) device.

5.3.1 Ag_2O powder

The first welding agent based on Ag used in this work to join YBCO single domains was the Ag_2O in powder. The decomposition of this material in air occurs at a temperature of 380°C according to the reaction:

$$Ag_2O \longrightarrow 2Ag + 0.5O_2 \tag{5.1}$$

The thickness of the Ag_2O powder suspension used in this study spanned the range 50 to 150μm. The powder was cold pressed to form a thin pellet and by using a suspension with acetone it was inserted between the two YBCO surfaces

to be welded. The microstructure of the final joints has been studied by using SEM.

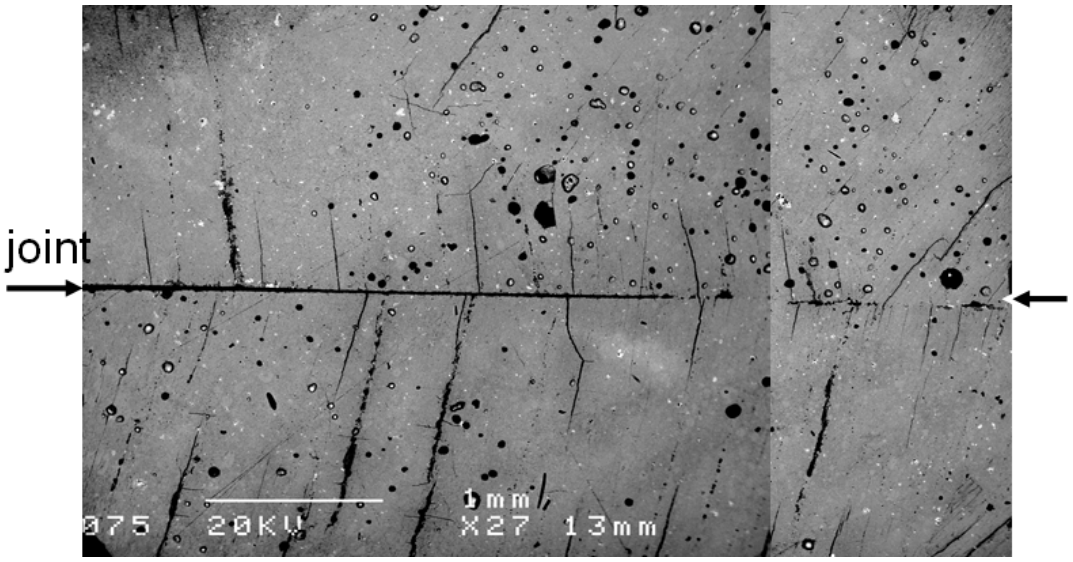

Figure 5.5: SEM micrograph corresponding to the ac plane of a joint obtained by using a 50μm thick Ag_2O suspension. Arrows indicate where the joint is.

In figure 5.5 it is represented a general view of the microstructure of the joint obtained by using a $\simeq$50μm thick Ag_2O suspension. The plane analyzed is the ac plane and the joint is indicated in the figure by arrows. It is obvious that the grains are badly connected between them and that the sample is very porous and with cracks which change direction while crossing the junction, thus indicating that the crystallographic orientation is different at both sides of the joint.

A higher magnification of different areas of the joint shows that there are zones where the YBCO grains are not connected and zones where the connection is better. In figure 5.6a it is observed that the interface shows an abundant porosity. The porosity observed at the interface by SEM macrographs is due to the fact that the initial density of the Ag_2O is low and then a big amount of residual porosity is formed at the interface. This porosity reduces the superconducting properties of the final joints, thus, representing an important limitation factor for the use of the Ag_2O powder as welding agent. Figure 5.6b shows that

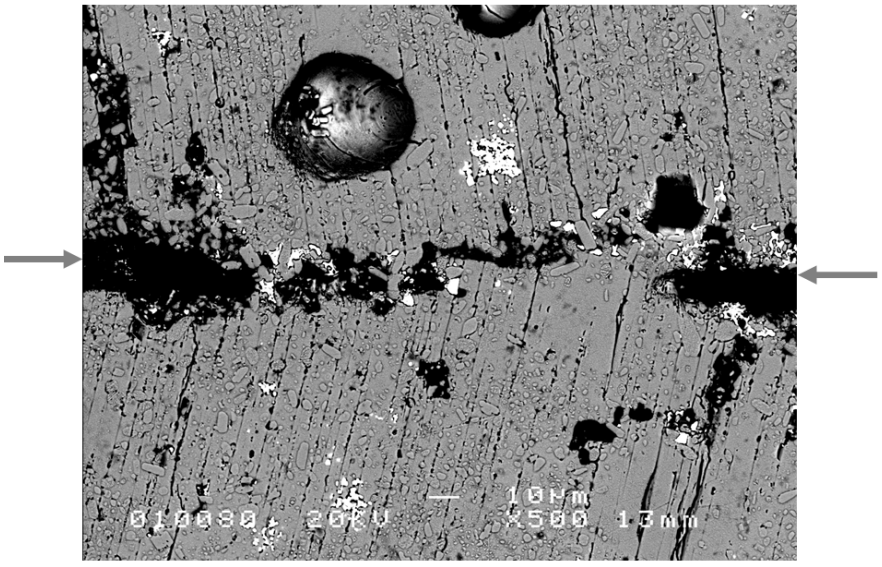

(a)

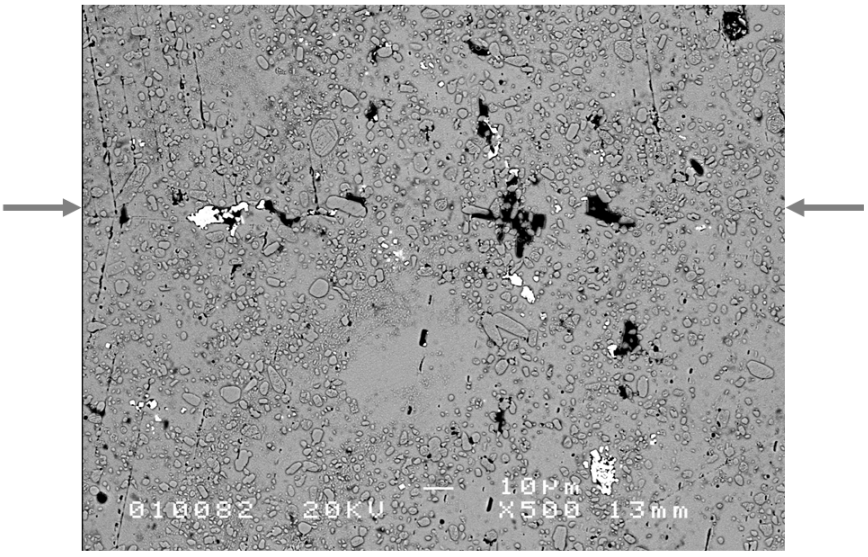

(b)

Figure 5.6: SEM micrograph of an ac plane of a joint when the welding agent is a ≈ 50 μm thick pressed Ag_2O powder: a) an abundant porosity is observed; b) a better connectivity between grains is achieved but some porosity still can be seen. The interface is indicated by arrows.

the connection between grains is improved but still some porosity can be seen around the joint area. In both images a large misorientation of the cracks while

crossing the weld is observed. It is very likely, then, that both YBCO single domains have nucleated independently from the molten interface and so the weld, when it is properly connected, is actually a large angle grain boundary and it will have in any case low critical currents.

5.3.2 Ag thin foil

Because of the limitations already mentioned when using pressed Ag_2O powder as welding agent to joint YBCO monoliths, i.e the porosity resulting at the interface and the difficulty to obtain a good contact between both pieces, another welding agent based on Ag has been investigated in this work: a metallic Ag thin foil obtained by a standard cold rolling process. This method offers two advantages: 1) between the YBCO single domains and welding agent exists a better contact which is very important for a good welding; 2) no porosity is introduced initially at the interface.

Thus, two YBCO tiles were cut with the geometry indicated in figure 5.2 and the two surfaces to be joint were polished down to a roughness of about 1μm. A metallic Ag foil with a thickness of about 50 μm was inserted between both tiles and the whole assembly was subjected to a thermal cycle as that indicated in figure 5.4, where T_{max}=1007°C, t_1=3h, T_2=990°C, t_2=1h, T_3=950°C and t_3=0h. Finally, the oxygenation process was carried out during t_{ox}= 120h at T_{ox}=450°C.

Figure **??** displays a SEM micrograph showing the microstructure of the whole area of a $\{100\}$ plane of a YBCO/Ag/YBCO interface welded using a 50 μm Ag foil. The joint is indicated in the figure by arrows. The first observation on this micrograph is that the welding immediately appears mechanically sound and has effectively occurred. Observations at higher magnification of the ab plane are represented in figure 5.8. Neither residual porosity nor chemical segregation could be observed throughout all the interface. This indicates that a perfect self-seeding process occurred with a final composition very close to that of the starting YBCO composite.

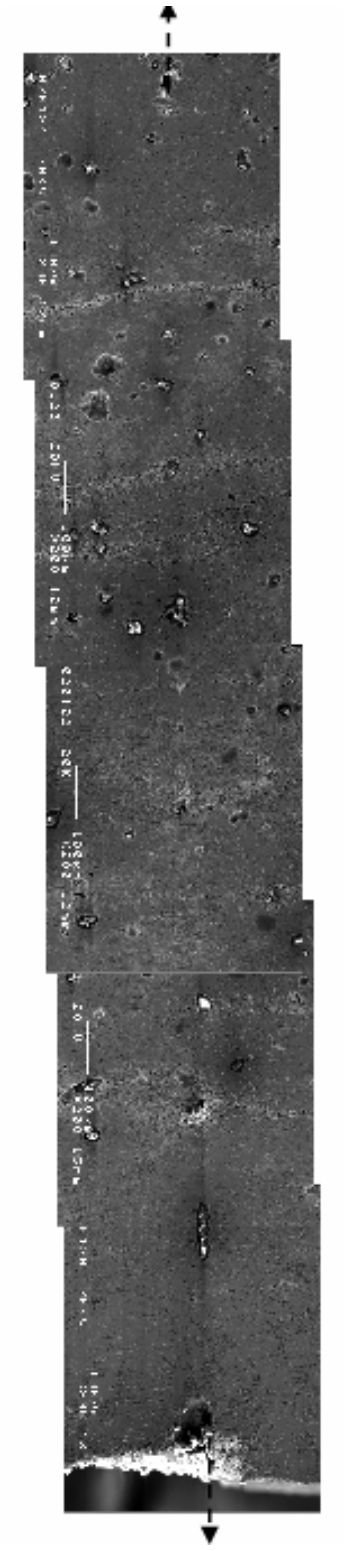

Figure 5.7: SEM micrograph showing a general view of the microstructure of the ac plane of the joint obtained by using a 50μm Ag foil. The joint is indicated by the arrows.

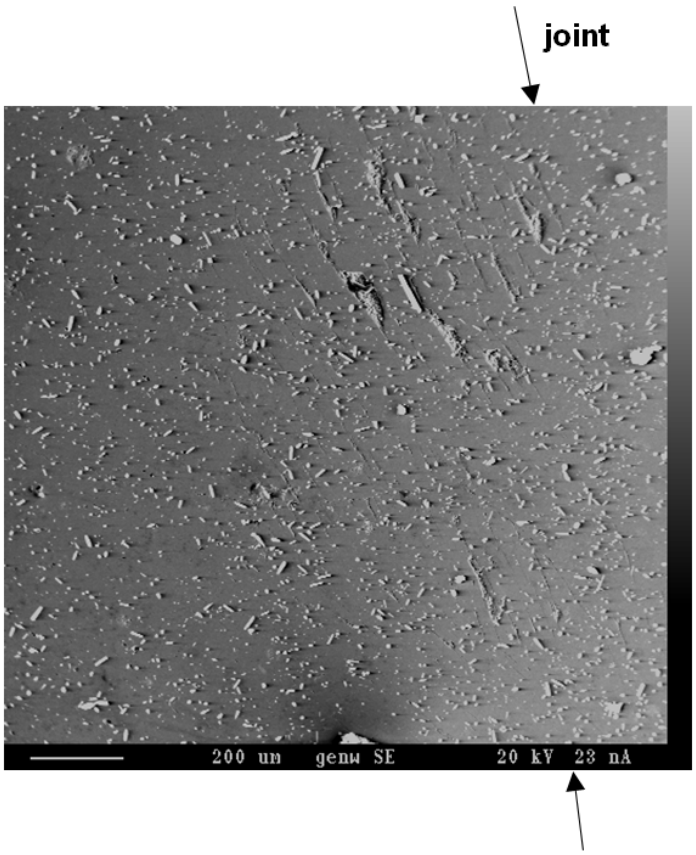

Figure 5.8: Observation at higher magnification of the ab plane of the joint area by using BSE. A perfect continuity is reached without porosity and non-superconducting phases. The joint is indicated by arrows.

A simple method used to observe the orientation of both single domains submitted to the welding process has been employed for the first time when the welding agent was Ag_2O powder (see figure 5.6). This method consisted in analyzing the orientation of the microcracks lying parallel to the ab plane across the joint. The angle formed by the microcracks existent in both YBCO parts to be joint gives the misorientation angle between the single domains. The visibility of these cracks can be low and is caused by "filling-up" the microcracks with fine particles of the sample created during the polishing process at the sample surface. This "filling" material was removed by a chemical etching process. The

etching consists in submerging the sample for 60 seconds in acetic acid, 10% diluted and after cleaned using ethanol. In this way a better observation of the microcraks is possible.

For this study a higher magnification of the (001) plane is performed. The sample was etched as it was mentioned before. The arrows in the figure indicate the interface. Note in figure 5.9 the continuity of microcracks across the joint which indicates that the ab planes are parallel in both YBCO monoliths.

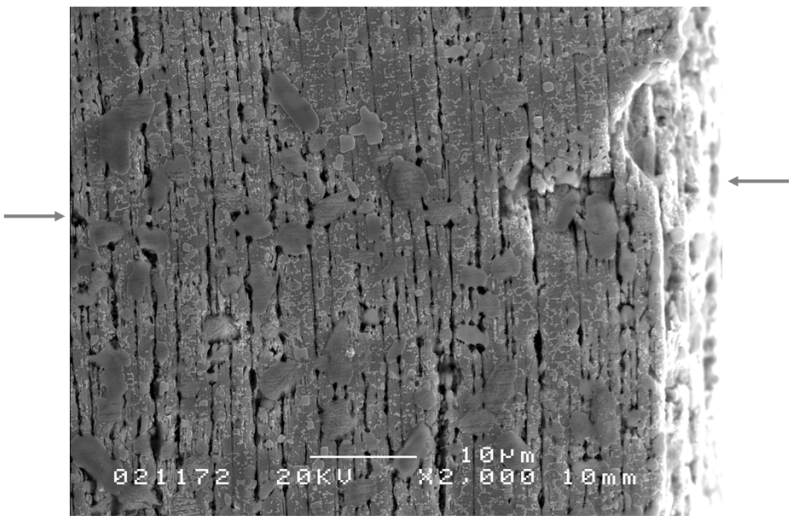

Figure 5.9: SEM image of a {100} plane of an YBCO/Ag/YBCO joint where a perfect matching of the two YBCO monoliths is observed without any sign of segregated metallic Ag at the interface. The arrows in the figure indicate the welding interface.

The quality of the superconducting joints obtained by this method has been demonstrated by means of Hall probe magnetic imaging and magnetoresistance measurements performed with fields up to 9T [68]. Figure 5.10 shows typical local magnetization M(x, y)=B(x, y)-μH images obtained after a field-cooled process under a magnetic field of 5000 Oe employing Hall microprobes at 77K. The sample has a parallelepiped geometry and dimensions of 3.8x2.2x4.9mm^3 and the joint is indicated in the figure by arrow. The magnetic field is applied parallel to the c-axis of the sample and parallel to the joint. It is observed that the shape of the profile is very sharp and pyramid-like. This means that there is no

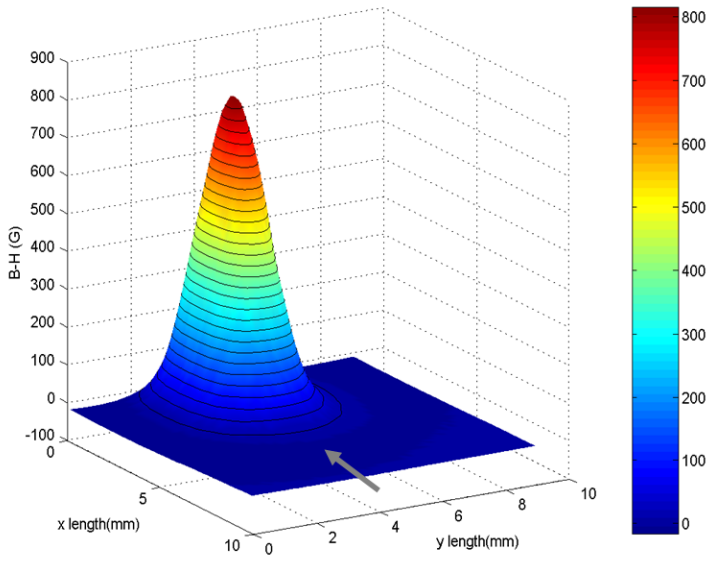

Figure 5.10: In-field Hall microprobe remanent magnetization profile after a field-cooled process of a joint YBCO sample with the interface and applied magnetic field parallel to the [001] axis. The remanent magnetization at the center of the joint is of $M_{rem}\simeq$800 Gauss. The joint is indicated by arrow.

decrease of the remanent magnetization at the weld, as it is typically observed in artificial joints with reduced critical currents [16,69]. Additionally, the remanent magnetization at the center of the joint is of $M_{rem}\simeq$800 Gauss, which is a good value for samples having these dimensions.

The critical current density of this sample has been determined from the Hall probe imaging measurements after a fc process and employing the software "Caragol" described in Chapter 3. As it was mentioned, this programme solves the inverse problem. It has been found that the J_c^{gb}=1$\times 10^4$ A/cm^2 at 77K in zero field when the external magnetic field is applied parallel to the c-axis of the sample and to the joint simultaneously.

The sample chosen to be measured by magnetoresistance has been cut in a parallelepiped form with a larger surface of the order of 1mm$\times$0.5mm, which coincides with the ab-plane. Afterwards, in order to enhance the sample resistance

and the sensibility of the measurements, the sample has been polished down to a thickness of 200 μm.

The sample resistivity has been determined by the 4 probe method. In this method, a current is applied through the external electrical contacts. In figure 5.11 it is represented the geometry arrangement of the contacts. The dark

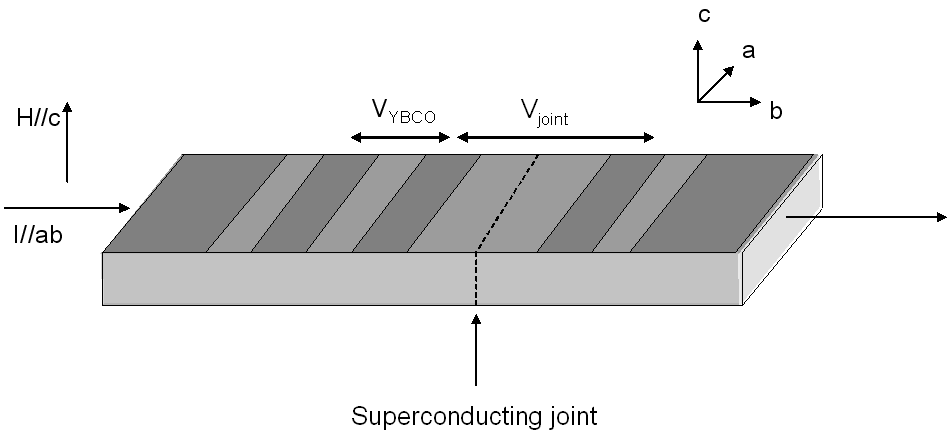

Figure 5.11: Geometry arrangement for the magnetoresistance measurements. Dark grey areas represent the contacts. The junction is indicated in the figure by dash line. The magnetic field is applied parallel to the c-axis and to the joint. The current is injected parallel to the ab plane and perpendicular to the joint.

grey areas indicate the contacts. The joint is indicated by the dashed-line in the figure. Thus, 5 platinum wires are attached to the sample by using silver epoxy. Afterwards, the sample is submitted to an annealing at the temperature of T=300°C during t=1h, under 1 bar of flowing oxygen to ensure low contact resistance contacts and no oxygen is lost from the sample. In this way a low resistance metallic contact between the sample and the wire is achieved.

Figure 5.12a displays magnetoresistance measurements performed with applied fields of 0.1T, 1T, 3T, 6T and 9T, with the magnetic field parallel to the c-axis and parallel to the joint and the current of I=5mA parallel to the ab plane (see figure 5.11). The field-dependent broadening typically observed in YBCO single crystals and single domain melt processes YBCO [70, 71] is also found in

the present case. However, it is important to note that no additional "foot" structure is observed coming from the joint which evidences the high quality of the superconducting joint [10]. Figure 5.12 shows the corresponding irreversibility lines defined with the criterion of ρ/ρ_n=5 $\times$ 10^{-3}, where ρ_n is the normal state resistivity at 95K. Notice that the irreversibility lines of the grains and joint follow the same power law relationship within the experimental error:

$$H_{irr} = H_0(1 - T/T_c)^{\alpha} \tag{5.2}$$

with H_0=113T and α=1.37. The resistivity and irreversibility line results allow us to conclude that there is no evidence of any degradation of the superconducting properties at the joint, even under magnetic fields as high as 9T, thus confirming that the welding process is of a very high quality.

In conclusion, considering the quality limitations found with the use of oxide silver powder as welding agent and the promising results achieved using Ag thin foils, we have abandoned the use of Ag_2O powder and we scheduled a systematic study of the YBCO joints parameters by using Ag thin foils as welding elements obtained by a cold rolling process.

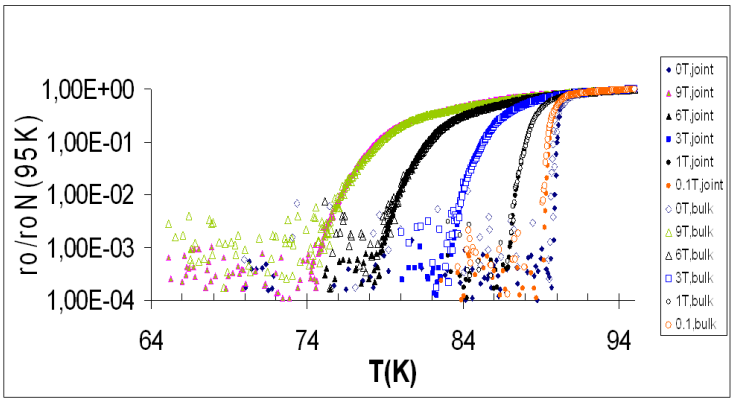

(a)

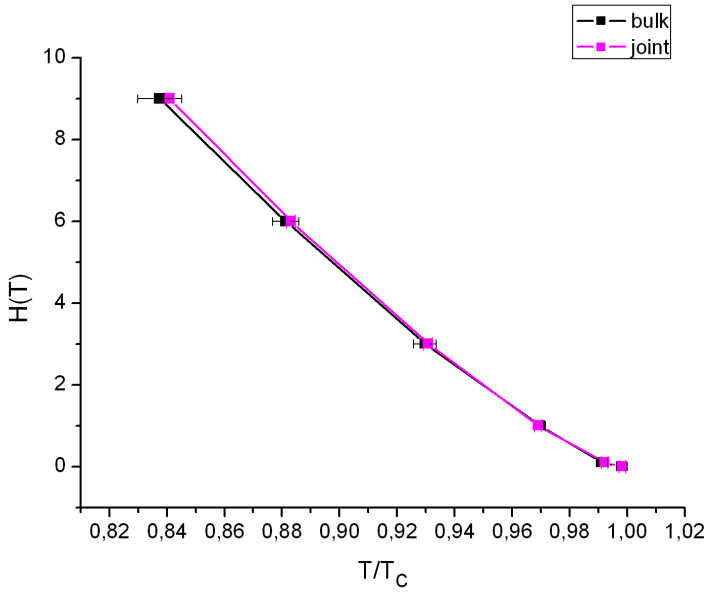

(b)

Figure 5.12: a) Temperature dependence of the magnetoresistance measured in fields of 0, 0.1, 1.3, 6 and 9T, applied parallel to the c-axis, of a single domain and to the joint. b) Irreversibility lines measured for the grain and for the final joint at the same time: black line for the bulk and magenta line for the weld.